



AALBORG UNIVERSITY
DENMARK

Aalborg Universitet

DC/DC Conversion and Distributed Grid based Solution of HVDC Tapping

Zhang, Qi; Silva, Filipe Miguel Faria da; Irnawan, Roni; Mochamad, Rian

Published in:
CIGRE Paris Session 2024

Creative Commons License
CC BY 4.0

Publication date:
2024

[Link to publication from Aalborg University](#)

Citation for published version (APA):

Zhang, Q., Silva, F. M. F. D., Irnawan, R., & Mochamad, R. (in press). DC/DC Conversion and Distributed Grid based Solution of HVDC Tapping. In *CIGRE Paris Session 2024* (pp. 1-14). Article 11593 CIGRE (International Council on Large Electric Systems).

General rights

Copyright and moral rights for the publications made accessible in the public portal are retained by the authors and/or other copyright owners and it is a condition of accessing publications that users recognise and abide by the legal requirements associated with these rights.

- Users may download and print one copy of any publication from the public portal for the purpose of private study or research.
- You may not further distribute the material or use it for any profit-making activity or commercial gain
- You may freely distribute the URL identifying the publication in the public portal -

Take down policy

If you believe that this document breaches copyright please contact us at vbn@aub.aau.dk providing details, and we will remove access to the work immediately and investigate your claim.

11593**B4 DC systems & power electronics
PS1 DC equipment and systems****DC/DC Conversion and Distributed Grid based Solution of HVDC Tapping****Qi ZHANG***
Aalborg University
Denmark
qzg@energy.aau.dk**Filipe Faria DA SILVA**
Aalborg University
Denmark
ffs@energy.aau.dk**Roni IRNAWAN**
Gadja Mada University
Indonesia
roniirawan@ugm.ac.id**Rian FATAH**
Gadja Mada University
Indonesia
rianfatahm@gmail.com**SUMMARY**

The increasing demand for efficient and reliable energy transmission solutions has underscored the significance of High Voltage Direct Current (HVDC) technology in modern power systems. HVDC systems have proven instrumental in addressing challenges such as offshore electricity transmission, interconnection of archipelagic nations, and long-distance power transport. However, the need for innovative approaches to address specific challenges, such as connecting multiple islands' energy systems, has led to the exploration of HVDC tapping as a potential solution. HVDC tapping, a concept analogous to different voltage levels in interconnected AC grids via power transformers, presents a promising approach for connecting multiple islands' energy systems. This concept involves the utilization of a DC/DC conversion method to reduce the voltage of the main HVDC link and transmit a small portion of its nominal power. The limitations in power magnitudes and the remote locations of tapping stations introduce operational and maintenance challenges, emphasizing the need for cost-effective, reliable, and user-friendly tapping converters.

To address these concerns and fill the research gap in HVDC tapping, this paper proposes an HVDC tapping solution containing a DC/DC converter and a related DC distribution system. The proposed solution incorporates a Modular Multilevel Converter (MMC) and a diode-bridge rectifier connected by a medium frequency transformer, offering cost advantages and ease of control. Furthermore, a DC distribution grid is utilized for connecting several islands at the low voltage side, with a novel control system for the DC/DC converter to ensure the stability of the low-voltage DC grid. The significance of this study lies in addressing the challenges associated with connecting decentralized and geographically intricate power systems, with a specific focus on the potential of HVDC technology in the context of the HVDC GREEN project. The proposed HVDC tapping solution can enhance power quality, and voltage stability of islands' power system. The study also presents novel fault-ride-through (FRT) control strategies to enhance the reliability of the DC distribution system, enabling the DC/DC converter to function as a current source during fault conditions, thereby preventing power outages.

KEYWORDS

High voltage direct current (HVDC) system, DC/DC conversion, HVDC tapping, Fault ride through control, converter control, island power system.

I. Introduction

HVDC-VSC links serve as pivotal transmission technology in the pursuit of energy system decarbonization, facilitating the transmission of substantial offshore-generated electricity to onshore locations, connecting archipelagic nations, and enabling the efficient transport of electricity over long distances. This technology is poised to play an increasingly vital role in the coming decades, with a projected surge in the number of HVDC links [1].

Indonesia's power system is intricately divided into independent segments characterized by diverse voltage levels, topologies, and power sources due to unique geographical conditions. The decentralized nature of this setup poses challenges to the stability and reliability of the country's power grid [2-4]. Despite the abundant potential for renewable energy, Indonesia's goal of transitioning from coal faces hurdles related to integrating renewable sources, including issues with weak grids, long-distance transmission, and the unpredictable nature of renewable generation [2-4]. The vast expanse of small islands in Indonesia, many located far from larger land masses, relies on small-scale, delicate power systems that grapple with stability and power quality challenges, which are required to be overcome by economic and societal development [2-4]. To address these challenges, Aalborg University (AAU), Universitas Gadjah Mada (UGM), and the Indonesian Electric Power Company PLN have collaborated in the HVDC GREEN project [4], aimed at exploring the interconnection of independent power systems through HVDC technology and investigating HVDC power tapping technology to support island power systems [5].

HVDC tapping technology aims to transmit a controllable, small amount of power either unidirectionally or bidirectionally from an HVDC transmission line to a local power system, serving the purpose of support, or collection of distributed energy. The concept of HVDC tapping is first reported in [6]; a solution based on motor and generator was proposed to tap a small amount of power from the HVDC link. Afterwards, in the next couple of years, several papers were published to discuss different solutions for HVDC tapping, and HVDC tapping technology was utilized in a real-world HVDC project, named Sardinia-Corsica-Italy [7]. These studies have proved the advantages of HVDC tapping technology and laid the foundation for subsequent research on HVDC tapping technology. In recent years, modular multilevel converters (MMC) have garnered attention for their outstanding modularity, flexibility, and scalability, making them particularly suitable for HVDC tapping applications. The literature has documented various applications of MMC in high and medium voltage HVDC tapping scenarios, classified primarily as isolated and non-isolated applications. Additionally, resonance-based DC/DC converters [8] have been explored for HVDC tapping, but their inherent challenges, such as modularity and scalability, remain significant obstacles.

Several publications [10-12] have reported on non-isolated MMC topologies for DC/DC conversion. These converters, employed for interconnecting DC grids, are transformer-less High Voltage DC-DC converters. In these converters, the arm AC circulating current of the MMC converter is utilized to balance submodule capacitor voltages while transferring DC power to the low-voltage side to achieve voltage conversion. However, the existence of arm circulating current necessitates additional LC filters to prevent AC circulating current injection into the DC output side [9-11]. Furthermore, the presence of AC circulating current reduces the energy conversion efficiency of the converter, and its magnitude increases with the rise in the input-output voltage ratio, limiting its application in high voltage ratio HVDC tapping [9, 12]. Moreover, the non-isolated converters impose similar grounding configurations for local low-voltage systems and high-voltage systems, constraining their potential applications in HVDC tapping.

Isolated topologies based on MMC have been suggested for HVDC tapping applications [13-20], aiming to achieve a high voltage ratio, enhanced efficiency, and isolation. The isolated topologies are typically DC/AC/DC, and medium or high frequency is used for the AC voltage to reduce the size of the transformer [14-19]. This two-stage DC power converter, represented by the dual active bridge converter, has been developed for many years, and the technology is relatively mature. But medium and high voltage HVDC tapping applications have put forward new requirements for this type of converter, such as higher requirements for modularity, economy, and reliability. According to the existing

literature, this type of converter can be divided into three-phase sine wave-based [6, 13, 19], single-phase sine wave-based [20], and single-phase square wave-based converters [14, 21] according to the form of AC voltage. References [6, 13] reported DC/DC converters using three-phase sine waves as intermediate stages based on MMC and discussed their application in HVDC tapping. The cost problem caused by using too many MMCs seems to be the biggest shortcoming of this type of converter, so the literature [14-15] discusses various improvements of this type of converter to reduce the number of MMC submodules. Literature [20] proposed a single-phase sine-wave-based DC/DC converter. The simple topology and the accompanying economy make this type of converter attractive. However, in order to eliminate the DC bias of the transformer, the transformer used in this conversion must be specially modified, and its core must contain an air gap. This need to customize the transformer greatly limits the application of this converter. A medium-frequency transformer has been employed, but square-wave modulation techniques were utilized, resulting in high dv/dt stress at the transformer terminals. Trapezoidal medium-frequency modulation techniques, as proposed in [17] and [18], were introduced to minimize dv/dt stress at the transformer terminals by applying sinusoidal voltage waveforms on the transformer primary.

The assessment in [9] highlights several critical issues in the current state of HVDC tapping technology. Firstly, it emphasizes the inadequacy in effectively blocking faults that may occur either on the main HVDC link or the low voltage side—a crucial requirement for HVDC tapping. Additionally, the review underscores concerns related to the design of the necessary inductor and the associated costs of the DC/DC converter, which pose as limiting factors. Considering these observations, it is evident that the existing converters, while applicable for HVDC tapping, fall short in terms of cost-effectiveness, reliability, and convenience. This necessitates the development of a converter that is not only more economically viable but also more reliable and user-friendly. Moreover, the context of HVDC tapping involves handling power flows of moderate magnitude, often in remote regions where tapping stations are situated. The limitations in power magnitudes translate to reduced economic advantages, while the remote locations introduce operational and maintenance challenges. As a result, HVDC tapping converters exhibit a heightened sensitivity to considerations of cost, reliability, and simplicity. Therefore, addressing these concerns becomes imperative for the advancement of HVDC tapping technology, ensuring its effectiveness in diverse operational scenarios, and facilitating its broader adoption in the energy sector. Moreover, most current research focuses on the design of the converter, while ignoring the local low-voltage networking scheme, as well as the comprehensive design of the networking scheme and the overall converter.

To fill the research gap in HVDC tapping, this paper proposes an HVDC tapping solution containing a DC/DC converter and the related DC distribution system. The DC/DC converter consists of MMC, and a diode-bridge rectifier connected by a medium-frequency transformer. The use of a diode-bridge rectifier allows a cost reduction, simple operation and high-reliability. Furthermore, a DC distribution grid is utilized in the tapping solution to connect several AC islands on the low-voltage DC side. Firstly, this paper proposes a novel control for the DC/DC converter to control the low-voltage DC grid and to assure respective stability. Each island's AC power system will incorporate a grid-forming (GFM) inverter responsible for maintaining AC stability. Additionally, a pioneering fault-ride-through (FRT) control strategy is presented for the DC/DC converter to enhance the reliability of the DC distribution system. By employing the proposed FRT controller, the DC/DC converter can function as a current source during fault conditions, thereby preventing power outages. Finally, the proposed solution will be comprehensively evaluated for power efficiency, power quality, and voltage stability through simulation case studies.

II. Proposed HVDC Tapping Solution

The studied HVDC tapping system, as illustrated in Figure 1, includes a tapping DC/DC converter connected to the main HVDC link, forming a DC distribution system utilized to interconnect several island power systems through grid-forming inverters.

The primary HVDC link employed in the simulation originates from the CIGRE DC test system [22, 23], serving as a representation of the dynamic behavior inherent in a standard HVDC system. The

examination of HVDC tapping solutions necessitates a preliminary evaluation of their impact on the primary HVDC link, especially during fault conditions within the DC distribution system. Consequently, advanced control mechanisms to mitigate these effects are explored further in this project. Given that the advanced control of the main HVDC link remains an area of ongoing research, the simulation employs master-slave control to investigate the influence of the DC distribution system on the primary HVDC link. In the simulation setup, the master station assumes responsibility for maintaining the DC voltage of the HVDC link, while the slave station operates as a constant power source injecting a specified power into the HVDC link. The HVDC link voltage is fixed at 525 kV, and the injected power from the slave station is set at 400 MW in accordance with project specifications. The DC cable transmission line spans 200 km, with frequency dependent phase model cables implemented as introduced in [22]. As an illustrative example, power is tapped from the midpoint of the primary HVDC link.

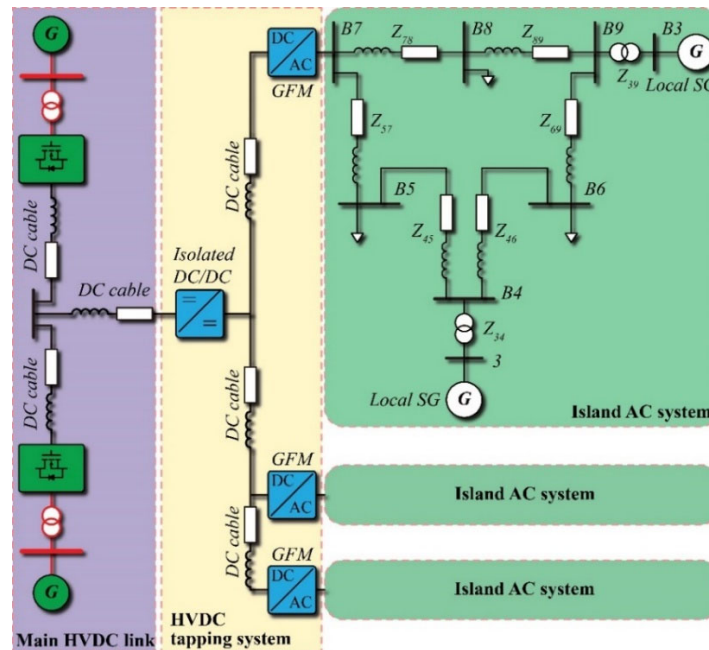


Figure 1 Illustration of the proposed HVDC tapping solution.

Local power systems on the islands are typically small and weak, relying on a limited power supply predominantly from fossil generation. In such cases, it proves advantageous for the main HVDC link to supply power to these systems through a grid-forming converter. A specific project objective involves devising an effective control strategy for the grid-forming converter (GFM) to ensure dynamic performance and stable voltage supply for the local weak system. Therefore, the local AC system, represented by a modified IEEE 9-bus system [24], typifies a small-scale power system. Firstly, the length of transmission lines in the standard system is reduced to make the system more consistent with the characteristics of small island power systems. Secondly, two generators connected to bus 9 and bus 4 are replaced with 10 MVA diesel generators, and the generator connected to bus 7 is replaced with a 20 MVA GFM inverter. Thirdly, loads in the system are reduced to 30 MVA in total.

Given the size and capacity of the local AC system, directly tapping power from the HVDC link at its normal voltage is deemed suboptimal due to potential cost implications associated with local GFM converters and additional DC cables necessitated by high voltage requirements. To address this concern, the project introduces a step-down DC/DC converter to reduce the voltage to a suitable level for power tapping. This isolated DC/DC converter operates at 525 kV on one side and 50 kV on the other. For simulation simplicity, only one local AC system is modeled using the IEEE-9 bus system [24], while the other AC systems are represented by GFM and fixed loads. The parameters of the modified IEEE-9 bus system are given in Table 1 and Table 2.

Table 1 Generator parameters of the modified IEEE-9 bus system.

Parameter	Value	Parameter	Value
Power	10 MVA	Xq'	0.25 p.u.
Voltage	6.3 kV	Xd''	0.25 p.u.
Ra	0.0015 p.u.	Xq''	0.312 p.u.
X0	0.15 p.u.	T'd0	5 s
X1	0.15 p.u.	T'q0	0.1 s
Xd	1 p.u.	T''d0	0.05 s
Xq	0.61 p.u.	T''q0	0.276 s
Xd'	0.32 p.u.	H	4 s

Table 2 Transmission line parameters of the modified IEEE-9 bus system.

Label	Length (km)	R0 (Ω/km)	L0 (mH/km)	C0 (pF/km)	R12 (Ω/km)	L12 (mH/km)	B12 (pF/km)
L4_5	8.993	0.59	3.98	5.89	0.059	1.33	9.81
L4_6	9.734	0.92	3.98	4.88	0.092	1.33	8.14
L5_7	17.0338	0.94	3.98	5.41	0.094	1.33	9.01
L6_9	17.986	1.15	3.98	5.99	0.115	1.33	9.98
L7_8	7.6176	0.59	3.98	5.89	0.059	1.33	9.81
L8_9	10.6646	0.59	3.98	5.89	0.059	1.33	9.83

The design of the HVDC tapping topology must take into consideration the requirements of the local low-voltage power systems. If there was only one local low-voltage system, a DC/AC converter would be a convenient solution. However, when multiple local low-voltage systems need to be connected to the HVDC system, an AC or DC distribution system must be designed to achieve interconnection. Nevertheless, there is limited discussion on whether an AC or DC distribution network is more suitable. This paper proposes a tapping solution based on a DC distribution network, considering the requirements of the HVDC Green project. The consideration of a DC distribution network structure is motivated by several key reasons.

Firstly, the HVDC tapping is designed for the interconnection of islands in Indonesia, where submarine cables are the only viable option for transmission lines. The cable system and its significant reactive power characteristics pose substantial challenges to the stable operation of an AC power system, requiring additional reactive compensation devices. Furthermore, as HVDC tapping connects the low-voltage side of multiple islands, each island having its independent power supply system, adopting an AC distribution network would couple the operational states and fault handling of these islands. In the event of a fault on one island, the others would be affected. In contrast, a DC distribution network with individual island GFM inverters would isolate the impact of faults, enhancing the stability and reliability of the low-voltage systems.

Lastly, considering that the cost of converters increases exponentially with the increase in input-output voltage, the price of a high-voltage inverter may surpass the total cost of several low-voltage converters. Thus, while adopting a DC scheme may involve using more inverters, the overall cost may not necessarily exceed that of a single high-voltage inverter. As discussed in this paper, the proposed solution incorporates diode rectifiers on the low-voltage side of the DC/DC converters, significantly reducing the design and manufacturing costs of the DC/DC converters. Taking all factors into account, a branching distribution network topology appears to be a favorable choice for HVDC tapping in Indonesia.

III. Converters and Control

A. HVDC tapping converter

The depicted DC/DC converter, as illustrated in Figure 2, integrates a half-bridge Modular Multilevel Converter (MMC), a power inductor, a transformer, and a diode-based rectifier. This system plays a crucial role in the production of a manageable, high-voltage, high-frequency AC voltage connected to the primary HVDC link. The subsequent step involves reducing this AC voltage to a lower level via the

transformer. The diode-based rectifier then converts the diminished AC voltage into a stable DC voltage, ensuring a consistent power supply for the local DC distribution grid.

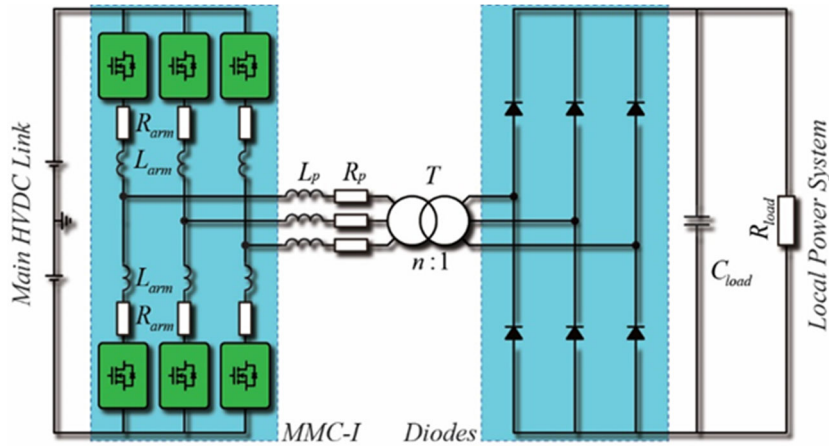


Figure 2 The topology of the proposed DC/DC tapping converter.

The control system depicted in Figure 3 for the DC/DC converter is designed with two closed loops: the inner current control loop and the outer DC voltage control loop. During steady-state operation, the output DC voltage from the diode-bridge rectifier remains constant. Consequently, the voltage difference across the AC inductor is solely determined by the output AC voltage of the MMC converter. The current control loop is designed accordingly, employing a PI controller to determine the amplitude of the AC voltage generated by the MMC converter based on the difference between the current amplitude reference and the measured current amplitude.

Due to the diode-bridge rectifier, the three-phase AC current is not a pure sine wave and contains numerous harmonics. To filter out these unwanted harmonics, a DSOGI-based bandpass filter is employed. Subsequently, the DQ transform is utilized to calculate the instantaneous amplitude of the three-phase current. The output DC voltage is controlled through the PI-based closed loop. However, owing to the diode rectifier, the output DC voltage exhibits voltage ripple, introducing disturbances to the closed control loop. To address this, a notch filter is implemented for DC voltage measurement, effectively filtering out the voltage ripple and enhancing the stability of the control loop. Table 3 outlines the key parameters of the proposed DC/DC converter.

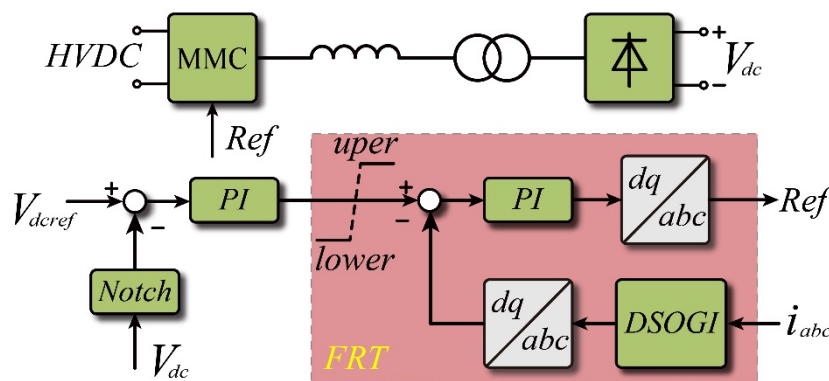


Figure 3 Block diagram of control system of the proposed DC/DC converter.

The double closed-loop control system, illustrated in the figure, offers the means to achieve fault ride-through capability for the converter. In instances where a fault arises on the DC side of the converter, the potential danger posed by excessive fault current to the power electronic converter is significant. The key to mitigating this risk lies in the effective control of converter current during a fault scenario, thereby enables fault ride-through capability. The incorporation of a current control loop is instrumental in this regard. This loop empowers the control system to manage the output current of the converter to any desired level, irrespective of whether the system is operating under normal conditions or

experiencing a fault. Consequently, the proposed control system inherently possesses fault ride-through capability, necessitating only the establishment of a predefined limit for the reference value of the current loop, such as 1.5 pu. This limit serves as a safeguard, ensuring that the current remains within acceptable parameters even in the event of a fault.

The proposed DC converter offers notable cost advantages attributed to the utilization of diode rectifiers. Leveraging the inherent commutation traits of diode rectifiers, this converter primarily necessitates control over the voltage amplitude and frequency generated by the MMC. Consequently, the complexity involved in designing the control system is significantly mitigated. Furthermore, the control system introduced in this study endows the DC converter with a remarkable low voltage ride-through capability. In the event of a fault occurring on the DC side, the converter seamlessly transitions, under the control system's guidance, into a current source operating mode. This mode enables the output of a steadfast amplitude current, furnishing essential fault support for the DC distribution system in the presence of faults. This adaptive feature reinforces the reliability and resilience of the converter in adverse operational conditions. The proposed converter, although not as flexible as the DAB converter and its output voltage has a 6-times frequency ripple, its prominent cost advantage makes it a very promising solution in HVDC tapping projects.

Table 3 Parameters of the proposed DC/DC converter.

Parameter	Value	Parameter	Value
Rate Power	50 MVA	MMC side AC Voltage	230 kV
HVDC voltage	525 kV	Rectifier side AC voltage	50 kV
Output DC voltage	50 kV	Frequency of AC voltage	400 Hz
Number of sub-models	200	Inductance of AC filter	10 mH
Arm Inductance of MMC	20 mH	Resistance of AC filter	0.1 Ohm
Equivalent resistance/arm of MMC	0.2 Ohm	Leakage Inductance of transformer	0.1 pu
Capacitance of sub-models	47 mF	Output smoothing capacitor	220 uF
Center frequency of notch filter	2.4 kHz	Resonant frequency of DSOGI	400 Hz
Kp of current controller	0.3	Kp of voltage controller	0.5
Ki of current controller	600	Ki of voltage controller	300

B. Grid forming inverter

Figure 4 depicts the topology and control block diagram for the GFM converter utilized in the simulation. The core circuit of the GFM converter includes a PWM converter that converts DC power to AC power through modulation, along with an LC filter responsible for smoothing the current injected into the power system. The symbols Z_l and Z_g denote the impedances of the transmission line and the connected power system, respectively. The control system of the GFM inverter, outlined in the figure, comprises three primary components: the current controller, voltage controller, and droop controller. The voltage and current controllers are interconnected to regulate the GFM inverter's output voltage to the reference value generated by the droop controller. It's essential to note that various GFM control strategies exist, but the GFM inverter illustrated in the figure represents the fundamental and typical approach. Additional GFM strategies can be achieved by incorporating extra control loops [25-27].

The structure of the droop, voltage, and current control loops is shown in Figure 5 [28, 29]. The current control loop includes the PI controller, voltage feedforward, and current decoupled element. The parameter tuning of the controller is based on making the entire system a typical first-order system. The parameters of the GFM inverter are shown in Table 4.

Table 4 Parameters of GFM inverter.

Parameter	Value	Parameter	Value
Rate Power	20 MVA	Ki of current controller	94.3
Rate AC Voltage	25 kV	Kp of voltage controller	5
Rate DC Voltage	50 kV	Ki of voltage controller	50
Capacitance of LC filter	22 uF	Active power droop coefficient	0.01
Inductance of LC filter	14.5 mH	Reactive power droop coefficient	0.005
Kp of current controller	3.1	Cutoff frequency of power filter	25 Hz

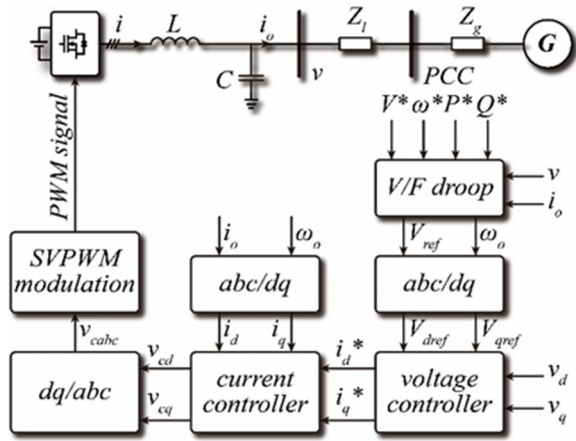


Figure 4 The topology and control block diagram of grid forming inverter.

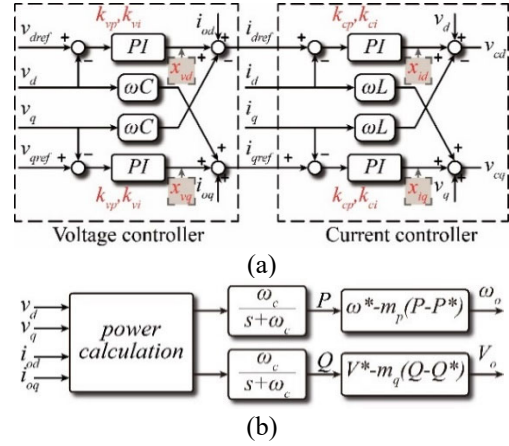


Figure 5 Control system of GFM inverters. (a) voltage and current control loops; (b) Structure of droop controller.

IV. Case Studies

To evaluate the effectiveness of the proposed scheme, a simulation-based test system for the envisaged HVDC tapping was meticulously constructed. This chapter is dedicated to elucidating the performance of the proposed HVDC tapping system, encompassing both the DC/DC converter and its associated control system, through a comprehensive case study. Initially, the focus is on a case study that delves into the operational characteristics of the converter itself. This entails a thorough exploration of the control system's proficiency in response to load variations and alterations in the output voltage. Subsequently, an examination of the proposed low voltage ride-through performance for the converter is conducted. In this scenario, the introduction of a fault into the DC grid allows for the observation of the dynamic behavior of the DC/DC converter, thereby illustrating its efficacy in maintaining operational integrity during low voltage conditions. Lastly, the dynamic performance of the proposed HVDC tapping system is scrutinized under varying conditions such as load fluctuations and AC system failures. Through these analyses, the adaptability and resilience of the proposed tapping system are effectively showcased, contributing valuable insights into its real-world applicability.

In order to reduce the complexity of the simulation system, the test system contains two low-voltage AC islands, one of which is represented by a GFM inverter and a modified IEEE9 BUS system, while the other island is represented by a GFM inverter and a fixed load, so there is only one AC Systems has internal dynamic characteristics.

A. Control performance (normal condition) of the proposed DC/DC converter

Figure 6 shows the steady-state performance and dynamic response of the proposed DC/DC converter. In the figure, "Vdc2_pu" denotes the per-unit value of the output DC voltage; "Iout_pu" denotes the per-unit value of the load DC current; and "Ipu" denotes the per-unit value of the three-phase AC current. Before 0.5s, the DC/DC converter works in a steady state, and it can be calculated from the output DC load current that the tapping power is 0.5 pu. The output DC voltage is very good, and no obvious ripple and oscillation appear under steady-state operation.

At 0.5s, a 10 MW load is added to the bus 6 of the modified IEEE 9-bus system. The output current of the converter reflects the increase in load, and the load current increases from 0.5 pu at steady state to 0.70 pu. The load step event increases the load current of DC/DC converter resulting in a very small voltage drop on the output voltage. The voltage control loop begins to increase the output power of the DC/DC converter, trying to compensate for the voltage drop. Therefore, a slight variation in the DC output voltage can be seen from the figure. The voltage variation caused by the load step is related to the parameters of voltage controller. In this case, the voltage variation is only 0.5 %, quite a small value

for the HVDC tapping requirements. Therefore, the performance of the proposed DC/DC converter fits the requirements of HVDC tapping applications.

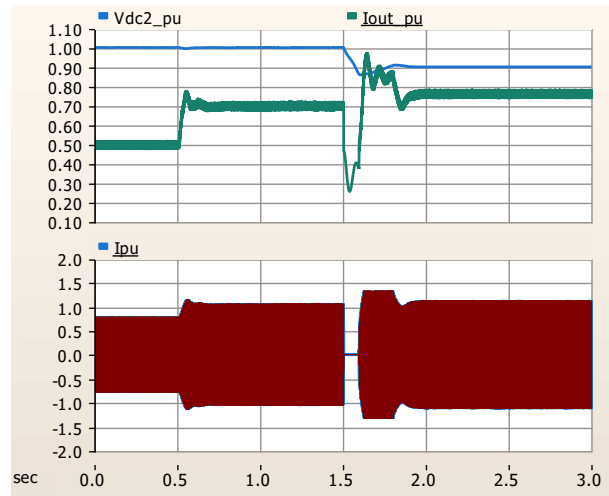


Figure 6 Performance of the proposed DC/DC converter in HVDC tapping application.

At 1.5s, the reference voltage is stepped down to 0.9 to present the dynamic response of the DC/DC converter. Because of diode-bridge, the power can only flow from MMC to the DC distribution system. The unidirectional nature of the energy flow in the converter precludes the reversal of energy when a step-down signal is applied to the control system. Consequently, the converter cannot absorb the energy that must be discharged from the capacitor in a reverse manner. In such instances, the converter can only cease supplying energy to the capacitor, leading to a free discharge until the voltage descends below the reference value. As illustrated in the figure, at the 1.5s mark, the output three-phase current from the converter abruptly reaches zero, signifying the cessation of energy supply to the capacitor. During this period, the capacitor undergoes free discharge against the load, causing a decline in voltage. Once the capacitor voltage dips below the reference value of 0.9 pu, the converter recommences current output, stabilizing the voltage around the specified reference value.

B. Fault ride through (FRT) of the proposed DC/DC converter

Figure 7 illustrates the fault ride-through performance of the proposed DC/DC converter. Initially, up to 0.5s, the converter operates in a steady-state condition. At 0.5s, a solid fault is introduced into the DC distribution system, specifically at the terminal connected to the GFM inverter for the modified IEEE-9 bus system. This fault induces a noticeable surge in the output of the DC inverter, causing a decline in the DC converter voltage. Upon the initiation of the fault, the control system promptly detects a voltage drop and responds by increasing the AC current to compensate for this decline. However, due to the substantial DC load current, the DC voltage continues to decrease. Once the AC current reaches its limit, the voltage controller is deactivated, and the output AC current is regulated to a constant amplitude, transitioning the converter into a current source operating mode. Notably, a post-fault observation reveals that the output DC current spikes to 2 pu. This overcurrent is attributed to capacitor discharge, leading to a subsequent decrease in the DC voltage. Approximately 1s after the fault occurrence, the output DC current stabilizes at 1 pu.

The findings from the presented results allow for the conclusion that the DC/DC converter exhibits fault ride-through (FRT) capability. This FRT capability proves pivotal as it enables the DC converter to mitigate disturbances in the main HVDC link when a fault arises in the local DC system, as shown in the sub-figure (b). This is especially significant for HVDC tapping converters, given the stringent requirements for security and reliability in the primary HVDC link. Additionally, the constant current output capability of the converter enhances its suitability for supporting HVDC tapping across diverse AC systems. The consistent output current facilitates power and voltage support for the healthy segments of the system.

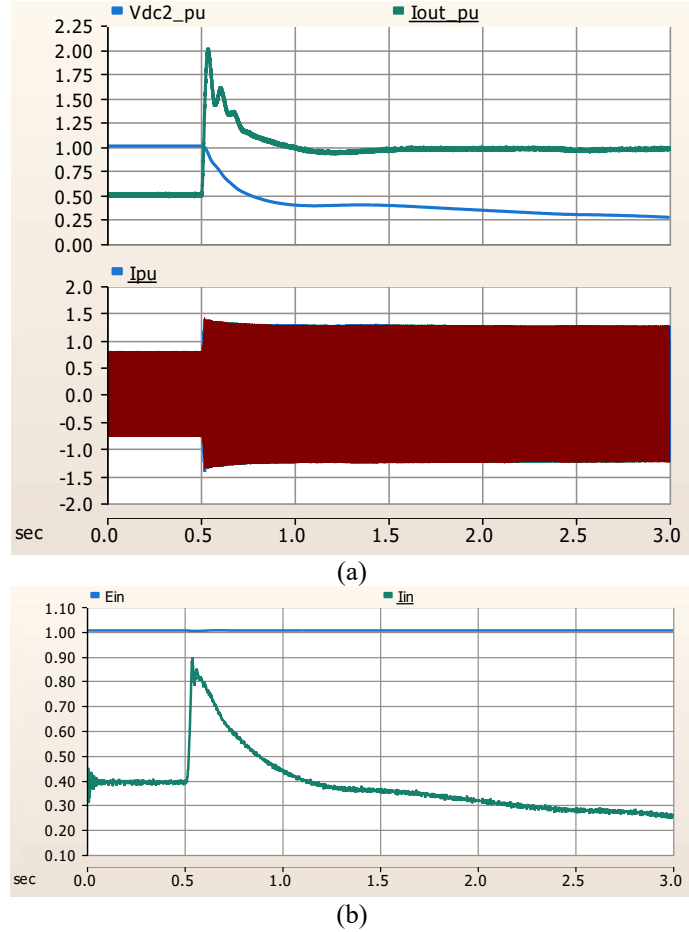


Figure 7 Fault ride through of the proposed DC/DC converter. (a) Output DC voltage, current and AC current of the DC/DC converter. (b) Voltage and current of the main HVDC link.

C. Performance of the DC distribution system in HVDC tapping application

To assess the performance of the DC distribution system, this subsection conducts case studies, focusing on the measurement of terminal voltages and currents in per-unit values. Additionally, the bus voltage, frequency, and output power of GFM inverters and two generators are monitored to illustrate the dynamic response of the modified IEEE-9 bus system. In the initial case study, load steps are systematically applied to the modified IEEE-9 bus system, simulating dynamic responses in both the DC and AC systems. Two distinct scenarios are considered within this case study: one involves a load increase, while the other simulates a load decrease. The amplitude of each load step is set at 10 MW, and these load steps are introduced at bus 6 within the modified IEEE-9 bus system. The second case study is designed to capture the response of both the DC and AC systems in the event of an AC fault. This scenario provides insights into the system behavior during abnormal AC conditions. By employing these case studies, the study aims to comprehensively evaluate and validate the performance of the DC distribution system under various dynamic scenarios, providing valuable insights into its robustness and reliability.

In the ensuing discussion, the symbols " V_{dc_t} ," " V_{dc_o} ," " V_{dc_1} ," and " V_{dc_2} " respectively represent the main HVDC link voltage, the DC/DC converter's output voltage, the DC terminal voltage of the GFM inverter connected to the modified IEEE-9 bus system, and the DC terminal voltage of the GFM inverter connected to a fixed load. Correspondingly, the symbols " I_{dc_t} ," " I_{dc_o} ," " I_{dc_1} ," and " I_{dc_2} " denote the DC currents. Additionally, " V_{b4} " to " V_{b9} " are symbols designating the bus voltages of the 9-bus system, while " w_{g4} ," " w_{g7} ," and " w_{g9} " represent the frequency at the AC terminal of the GFM and synchronous generators. Notably, all voltages, currents, and frequencies are expressed in per-unit values. Lastly, the symbols " P_{g4} " to " P_{g7} " are employed to denote the active power injected into the AC power system, with the unit of power measured in megawatts (MW). This comprehensive set of

symbols provides a clear and standardized representation of the various electrical parameters essential for the subsequent analyses and discussions within the context of the modified IEEE-9 bus system.

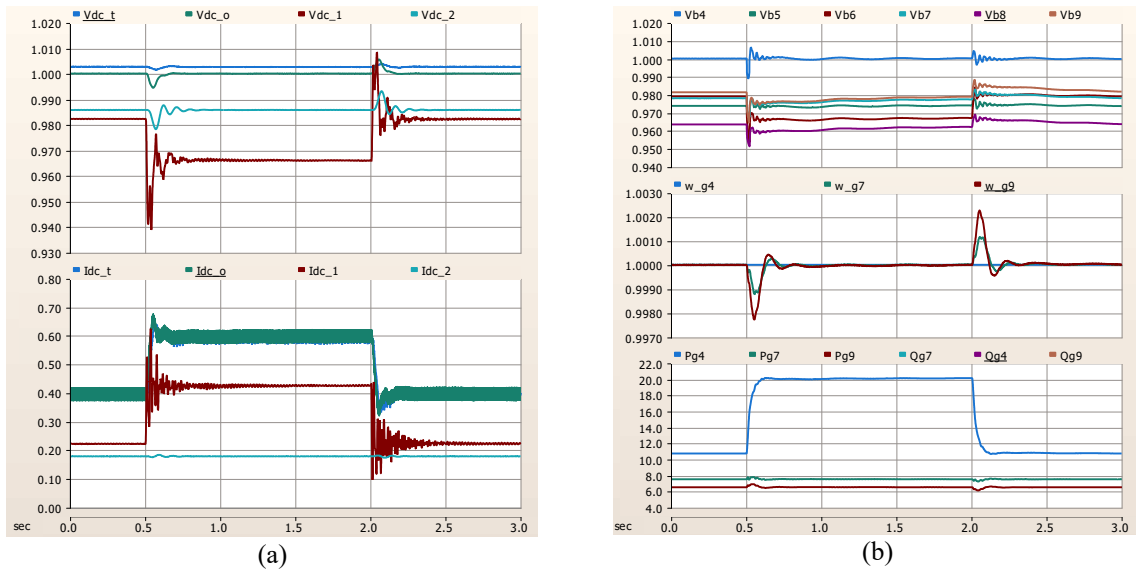


Figure 8 Response of DC and AC systems with load steps. (a) Response of DC distribution system (b) Response of modified IEEE-9 bus system.

Figure 8 illustrates the dynamic response of the HVDC tapping system when subjected to load step disturbances at 0.5s. Specifically, a 10 MW load is introduced to bus 6 within the modified IEEE-9 bus system. This load step induces an increase in DC current, subsequently leading to a DC voltage oscillation within the DC distribution system. Notably, the amplitude of this oscillation remains at approximately 1%, a level deemed acceptable for HVDC tapping applications. In the AC system, the load step triggers a frequency variation. It is essential to highlight that the GFM inverter employed in the system operates as an ideal voltage source, aims to provide a fixed output frequency of 50Hz for the AC system. Consequently, the additional power introduced by the load step is seamlessly accommodated by the GFM inverter, evident in the observed rise in the output power from 10.8 MW to 20 MW. To assess the system's performance during load shifting, the 10 MW load is removed at 2.0s. Subsequently, in sub-figure (b), it is evident that the output load promptly reduces to 10.8 MW. Throughout this process, the voltage, frequency, and output power demonstrate stability, remaining within acceptable ranges. Thus, Figure 8 serves as a valuable tool for evaluating the dynamic performance of the HVDC tapping system under varying load conditions.

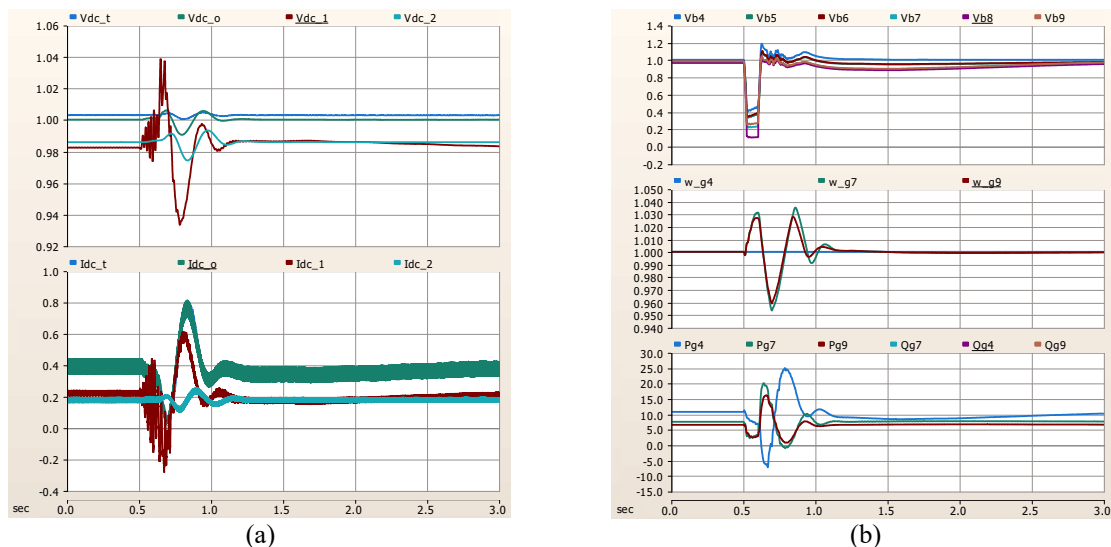


Figure 9 Fault response of the HVDC tapping system. (a) Response of DC distribution system (b) Response of modified IEEE-9 bus system.

Figure 9 depicts the response of the HVDC tapping system in the presence of a fault within the modified IEEE-9 bus system. In this scenario, a three-phase short-circuit fault is applied to bus 8 of the AC system, and the fault persists for a duration of 100 ms. Notably, this fault induces a substantial reduction in the bus voltage of the AC system. The inclusion of synchronous generators in the system amplifies the impact, leading to a pronounced frequency variation in the AC system. The fault also triggers power oscillations, further complicating the dynamic response. The resultant power oscillation introduces a discernible variation in the DC current, consequently affecting the DC voltage at the terminal connected to the GFM inverter. The amplitude of this oscillation is approximately 10% of the rated voltage. It is worth noting that the DC voltage at other terminals is marginally influenced by the fault due to the voltage regulation provided by the DC/DC converter. Despite the challenges posed by the fault, the system's design and control mechanisms contribute to mitigating the impact on the DC voltage at non-faulted terminals. This nuanced response underscores the robustness of the HVDC tapping system in managing and regulating voltages under fault conditions.

V. Conclusion

This paper introduces an innovative HVDC tapping solution designed to overcome the challenges associated with interconnecting decentralized and geographically intricate power systems, focusing on the HVDC GREEN project. The proposed solution, featuring an MMC-diode-bridge DC/DC converter and an associated DC distribution system, seeks to elevate power quality and voltage stability in HVDC tapping applications. Through extensive analysis and simulation studies utilizing a CIGRE DC test system and a modified IEEE 9-bus system, this research provides valuable insights into the performance and control strategies of the proposed HVDC tapping solution.

The novelty of this work lies in addressing the limitations of existing HVDC tapping technology by introducing a cost-effective, reliable, and easy-to-control tapping converter design. Moreover, a fault-ride-through (FRT) mechanism is proposed for the DC/DC converter, ensuring reliable operation during fault conditions, and the introduction of a DC distribution grid to interconnect multiple islands, presenting a comprehensive approach to HVDC tapping technology. This contribution advances the field of HVDC tapping technology and provides valuable insights for researchers, engineers, and policymakers involved in the integration of renewable energy sources and the enhancement of power systems, especially in challenging geographic regions. The research emphasizes not only the significance of optimizing converter design but also underscores the importance of designing the low-voltage side network for efficient operation in HVDC tapping applications. Overall, this paper highlights the potential of HVDC technology and emphasizes the need for a holistic approach in addressing the complexities of power systems in diverse environments.

BIBLIOGRAPHY

- [1]. Pierri, Erika, et al. "Challenges and opportunities for a European HVDC grid." *Renewable and Sustainable Energy Reviews* 70 (2017): 427-456.
- [2]. Ministry of Energy and Mineral Resources, "Indonesia Grid Code 2022 (Permen ESDM No.20 2020)," 2020. [Online]. Available: <https://jdih.esdm.go.id/storage/document/PM%20ESDM%20No%202020%20Tahun%202020.pdf>.
- [3]. Institute for Essential Services Reform, "Indonesia Energy Transition Outlook 2021," 2021.
- [4]. R. Inawan and F. M. F. da Silva, "The HVDC Green Handbook," Aalborg, 2022.
- [5]. Q. Zhang, F. F. da Silva, R. Inawan and R. F. Mochamad, "Control of MMC-based Isolated DC/DC converter for HVDC Tapping," 2023 IEEE Belgrade PowerTech, Belgrade, Serbia, 2023, pp. 1-6, doi: 10.1109/PowerTech55446.2023.10202693.
- [6]. Bowles, J. P., H. L. Nakra, and A. B. Turner. "A small series tap on an HVDC line." *IEEE Transactions on Power Apparatus and Systems* 2 (1981): 857-862.
- [7]. V B. Collet, J. Taisne, V. Arcidiacono and F. Mazzoldi, "The Corsican Tapping: from design to Commission Test of the third Terminal of the Sardinia-Corsica-Ity HVDC Link", IEEE

- Transactions on Power Delivery, vol. 4, no. 1, pp. 794-799, Jan 1989.
- [8]. E. C. Mathew, R. Sharma, and A. Das, "A Modular Resonant DC–DC Converter With High Step-Down Ratio for Tapping Power From HVDC Systems," *IEEE Trans. Ind. Electron.*, vol. 68, no. 1, pp. 324–332, 2021, doi: 10.1109/TIE.2020.2965473.
 - [9]. Paez, Juan David, et al. "Overview of DC–DC converters dedicated to HVdc grids." *IEEE Transactions on Power Delivery* 34.1 (2018): 119-128.
 - [10]. Kish, Gregory J. "On the emerging class of non-isolated modular multilevel DC–DC converters for DC and hybrid AC–DC systems." *IEEE Transactions on Smart Grid* 10.2 (2017): 1762-1771.
 - [11]. Ferreira, Jan A. "The multilevel modular DC converter." *IEEE Transactions on Power Electronics* 28.10 (2013): 4460-4465.
 - [12]. Hagar, Abdelrahman Abbas, and Peter W. Lehn. "Comparative evaluation of a new family of transformerless modular DC–DC converters for high-power applications." *IEEE transactions on power delivery* 29.1 (2014): 444-452.
 - [13]. D. Jovicic and H. Zhang, "Dual channel control with dc fault ride through for MMC-based, isolated dc/dc converter," *IEEE Trans. Power Del.*, vol. 32, no. 3, pp. 1574–1582, Jun. 2017.
 - [14]. S. Kenzelmann, A. Rufer, D. Dujic, F. Canales, and Y. R. de Novaes, "Isolated dc/dc structure based on modular multilevel converter," *IEEE Trans. Power Electron.*, vol. 30, no. 1, pp. 89–98, Jan. 2015.
 - [15]. B. Zhao, Q. Song, J. Li, Y. Wang, and W. Liu, "High-frequency-link modulation methodology of dc–dc transformer based on modular multilevel converter for HVDC application: Comprehensive analysis and experimental verification," *IEEE Trans. Power Electron.*, vol. 32, no. 5, pp. 3413–3424, May 2017.
 - [16]. H. Liu, M. S. A. Dahidah, J. Yu, R. T. Naayagi, and M. Armstrong, "Design and control of unidirectional dc–dc modular multilevel converter for offshore dc collection point: Theoretical analysis and experimental validation," *IEEE Trans. Power Electron.*, vol. 34, no. 6, pp. 5191–5208, Jun. 2019.
 - [17]. I. A. Gowaid, G. P. Adam, A. M. Massoud, S. Ahmed, and B.W. Williams, "Hybrid and modular multilevel converter designs for isolated HVDC–DC converters," *IEEE J. Emerg. Sel. Topics Power Electron.*, vol. 6, no. 1, pp. 188–202, Mar. 2018.
 - [18]. I. A. Gowaid, G. P. Adam, A. M. Massoud, S. Ahmed, D. Holliday, and B. W. Williams, "Quasi two-level operation of modular multilevel converter for use in a high-power dc transformer with dc fault isolation capability," *IEEE Trans. Power Electron.*, vol. 30, no. 1, pp. 108–123, Jan. 2015.
 - [19]. T. Lüth, M. M. C. Merlin, T. C. Green, F. Hassan, and C. D. Barker, "High-frequency operation of a dc/ac/dc system for HVDC applications," *IEEE Trans. Power Electron.*, vol. 29, no. 8, pp. 4107–4115, Aug. 2014.
 - [20]. Parida, Nibedita, and Anandarup Das. "Modular multilevel DC–DC power converter topology with intermediate medium frequency AC stage for HVDC tapping." *IEEE Transactions on Power Electronics* 36.3 (2020): 2783-2792.
 - [21]. X. Xiang, X. Zhang, T. Luth, M. M. C. Merlin, and T. C. Green, "A Compact Modular Multilevel DC–DC Converter for High Step-Ratio MV and HV Use," *IEEE Trans. Ind. Electron.*, vol. 65, no. 9, pp. 7060–7071, 2018, doi: 10.1109/TIE.2018.2793249.
 - [22]. Vrana, Til Kristian, et al. "The CIGRE B4 DC grid test system." *Electra* 270.1 (2013): 10-19.
 - [23]. CIGRE WG B4.58 and CIGRE WG B4.57, "The CIGRE B4 DC Grid Test System," *Electra CIGRE's digital magazine ELT_270_9*, 2013. [Online]. Available: https://e-cigre.org/publication/ELT_270_9-the-cigre-b4-dc-grid-test-system .
 - [24]. J. P. Berard, OPAL-RT: IEEE 9 Bus System Example. [Online]. Available: www.opal-rt.com .
 - [25]. J. Rocabert, A. Luna, F. Blaabjerg, and P. Rodríguez, "Control of Power Converters in AC Microgrids," *IEEE Trans. Power Electron.*, vol. 27, no. 11, pp. 4734–4749, 2012, doi: 10.1109/TPEL.2012.2199334.
 - [26]. R. Rosso, X. Wang, M. Liserre, X. Lu, and S. Engelken, "Grid-Forming Converters: Control Approaches, Grid-Synchronization, and Future Trends - A Review," *IEEE Open J. Ind. Applicat.*, vol. 2, pp. 93–109, 2021, doi: 10.1109/OJIA.2021.3074028.
 - [27]. X. Wang, Y. W. Li, F. Blaabjerg, and P. C. Loh, "Virtual-Impedance-Based Control for Voltage-Source and Current-Source Converters," *IEEE Trans. Power Electron.*, vol. 30, no. 12, pp. 7019–

7037, 2015, doi: 10.1109/TPEL.2014.2382565.

- [28]. Q. Zhang, D. Liu, and Z. Chen, "Fault Modeling of Grid-Forming Converters Using Dynamic Phasor Theory," in 2021 IEEE/IAS Industrial and Commercial Power System Asia (I&CPS Asia), Chengdu, China, 2021, pp. 1011–1016.
- [29]. Q. Zhang, D. Liu, Z. Liu, and Z. Chen, "Fault Modeling and Analysis of Grid-Connected Inverters with Decoupled Sequence Control," IEEE Trans. Ind. Electron., vol. 69, no. 6, pp. 5782–5792, 2022, doi: 10.1109/TIE.2021.3088378

The research is funded by the Ministry of Foreign Affairs of Denmark via the Danida Fellowship Centre with the project: "HVDC GREEN: HVDC Grid for Interconnecting Nusantara", project no. 20-M02AAU.